Green Chemistry

PAPER

View Article Online
View Journal

Cite this: DOI: 10.1039/d0gc03100c

Advances in bio-nylon 5X: discovery of new lysine decarboxylases for the high-level production of cadaverine†

Yaju Xue,[a] Yongliang Zhao,[a] Xiuling Ji,[a] Jiahao Yao,[a] Peter Kamp Busk,[c] Lene Lange,[d] Yuhong Huang *[a,b,e,f] and Suojiang Zhang *[a,b]

Cadaverine (1,5-pentanediamine) is the most important precursor for nylon PA5X, which has an extremely competitive market due to the high consumption of engineered plastics and fibers. The key enzyme lysine decarboxylase is in desperate need for industrial bio-based cadaverine production. In this study, new lysine decarboxylases have been mined by peptide pattern recognition for the high-level production of cadaverine. The predicted enzymes were expressed in *E. coli* and analyzed as whole-cell biocatalysts. Two outstanding recombinant enzymes from *Edwardsiella tarda* and *Aeromonas* sp. (LdcEt and LdcAer, respectively), were further purified and characterized. The optimal pH and temperature for LdcEt and LdcAer were pH 7, 55 °C and pH 6, 50 °C, respectively. These two enzymes were stable over the pH range of 5–7 during 24 h incubation. Both of them still had activity after being incubated at pH 8. LdcEt and LdcAer also have good thermostability with a half-life of 14.5 h and 20.3 h at 60 °C, respectively. The kinetic analysis showed that they have high catalytic efficiency as the k_{cat}/K_m (LdcEt: 243.28 s^{-1} mM^{-1}; LdcAer: 266.86 s^{-1} mM^{-1}) was the highest when compared for all the related studies. The whole cell conversion by LdcEt with 0.1% (v/v) Triton X-100 can convert 100% 2 M L-lysine HCl to cadaverine in 2 h and the cadaverine productivity was high up to 103.47 ± 4.37 g L^{-1} h^{-1}. The *in vitro* studies further found that unpurified cell-lysates of LdcEt had relatively higher activity compared to the whole cell conversion. Meanwhile, 0.4 mg mL^{-1} purified LdcEt and LdcAer can efficiently produce 165.96 ± 1.41 g L^{-1} and 155.84 ± 4.63 g L^{-1} cadaverine only in 0.5 h, respectively. The high specific activity, pH, thermo-stability, and catalytic efficiency *in vivo* and *in vitro*, combined with simultaneous cell treatment with Triton X-100 and the bioconversion process, provide LdcEt with great potential in the economic and efficient production of cadaverine at the industrial scale.

Received 12th September 2020,
Accepted 2nd November 2020

DOI: 10.1039/d0gc03100c

rsc.li/greenchem

Introduction

Nylon polyamides (PAs) are well-known lightweight and tough synthetic polymers, which have been widely applied in the automotive, engineering plastics, electronics and electrical, textile, and other industries.[1] The growing population and the presence of huge secondary processed product manufacturers have boosted the demand of the nylon market.[2] PA 66 is one of the most important and widely used nylon varieties as it has strong dielectric resistance in thermally- and mechanically-stressed moldings. In Europe and China, the shortage of the major raw material adiponitrile, which is the precursor of hexamethylenediamine for PA 66, has caused a price hike and put significant pressure on the supply.[3] Meanwhile, petroleum-based hexamethylenediamine has significant impact on the environmental sustainability. Therefore, similar and sustainable substitute products with good characteristics for PA 66 are highly expected to be explored. Bio-based nylon PA5X varieties (such as PA52, PA54, PA56, and PA510) are synthesized from cadaverine and diprotic acid by a green process, throwing light on the development of the renewable nylon market. It has been reported that bio-based nylon PA56 with

[a]*Beijing Key Laboratory of Ionic Liquids Clean Process, CAS Key Laboratory of Green Process and Engineering, State Key Laboratory of Multiphase Complex Systems, Institute of Process Engineering, Chinese Academy of Sciences, Beijing 100190, China. E-mail: yhhuang@ipe.ac.cn, sjzhang@ipe.ac.cn*
[b]*Innovation Academy for Green Manufacture, Chinese Academy of Sciences, Beijing 100190, China*
[c]*Department of Science and Environment, Roskilde University, Universitetsvej 1, 4000 Roskilde, Denmark*
[d]*BioEconomy, Research & Advisory, Copenhagen, 2500 Valby, Denmark*
[e]*Zhengzhou Zhongke Emerging Industry Technology Research Institute, Zhengzhou City, Henan 450000, China*
[f]*Zhongke Langfang Institute of Process Engineering, Langfang 065001, China*
†Electronic supplementary information (ESI) available. See DOI: 10.1039/d0gc03100c

remarkable properties such as lightweight, good moisture absorption, thermo-resistance, high tensile strength, low temperature dyeing, high elasticity, and flame retardancy has great potential to be developed into various high-end applications.[4]

However, recently, no market supplies of cadaverine (1,5-pentanediamine ($NH_2(CH_2)_5NH_2$)), which is the most important precursor for PA5X, has limited the further global production of PA5X. The petrochemical technology for cadaverine production is neither cost efficient nor economically viable at the industrial scale due to its low selectivity in catalysis and high-cost of the precursor.[2] Therefore, the efficient, green, and economic process for the high-level production of cadaverine is a primary issue for the PA5X market. Gale and Epps[5] firstly observed that lysine decarboxylase from *Escherichia coli* can be induced during the acid stress-induced process. This significant discovery has paved a shortcut for bio-based cadaverine production.

Currently, biocatalytic approaches for cadaverine production are inherently divided into fermentation and whole cell bioconversion. The former is beneficial for use in natural raw materials such as glucose,[6] cellobiose,[7] starch, and sucrose[8] and other related alternative carbon sources for the production of cadaverine by genetic *E. coli* or *Corynebacterium glutamicum* strains. However, the biotoxicity of the product and the released CO_2 limit the cell to maintain its viability and activity for growth and catalysis during the fermentation process, resulting in low yield of cadaverine (less than 100 g L^{-1}).[9] Meanwhile, the relatively low concentration of cadaverine, various cell-secreted metabolites, and residue compounds in the culture broth and the cellular degradation of the product have significant effects on the downstream purification of cadaverine. Whole-cell bioconversion, in turn, can directly convert L-lysine to cadaverine in a single step. This reaction process does not require complex fermentation control and there is no accumulation of the by-products. It has been expected that the global L-lysine market will be about 3.28 million metric tons and the price of L-lysine has decreased to about $1.5 in 2020.[10] Therefore, whole-cell bioconversion using recombinant strains with lysine decarboxylase is a promising and economic route for the direct conversion of L-lysine to cadaverine.

Most of the studies have focused on inducible lysine decarboxylase (EC 4.1.1.18) from *E. coli* (CadA) as it has high catalytic activity and expression level.[6,11] Ajinomoto Corporation took the lead in constructing genetically engineered strains; after overexpressing the *E. coli* lysine decarboxylase, the titer of cadaverine was up to 66.8 g L^{-1}.[12] Then, the introduction of lysine/cadaverine antiporter (CadB), fusing the signal sequence to the recombinant strains, has been confirmed for improving the mass transfer and increasing the production of cadaverine, such as *E. coli* BL-BADE (pETDuet-*pelB-cadB-cadA*)[13] and *E. coli* BL21Δ*spe*EΔ*puu*AΔ*spe*GΔ*ygj*G (pSITDuet-*cadA-pelB-cadB*).[14] Kanjee *et al.*[15] have revealed that CadA is an oligomer of five dimers, which associate to form a decamer. The structure of the decamer is sensitive when the pH changes from 5.0 to 8.0, which significantly affects the stability and activity of the enzymes. Therefore, it is necessary to improve the stability of CadA by protein engineering. Ajinomoto and Mitsui Chemicals Corporation have screened mutants with higher thermal stability and activity through the directed evolution of CadA.[16] Hong and Kou have half-rationally designed the decameric interface of CadA and the target mutants F14C/K44C/L7M/N8G and T88S obviously improved the stability and activity, which can produce 157 g L^{-1} cadaverine in 9.5 h (productivity: 16.52 g L^{-1} h^{-1}) and 198 g L^{-1} cadaverine within 5 h (productivity 40 g L^{-1} h^{-1}).[17,18] Pyridoxal phosphate phosphate (PLP) cofactor plays an important role in the catalysis of PLP-fold type I lysine decarboxylase CadA. Moon *et al.*[19] introduced an intracellular ATP regeneration system using polyphosphate kinase (ppk) into systems containing CadA and PdxY for intracellular PLP production and combined it with hexadecyltrimethylammonium bromide (CTAB) for membrane permeabilization, which resulted in 102 g L^{-1} cadaverine in 6 h (productivity: 17 g L^{-1} h^{-1}). Ma *et al.*[20] introduced intracellular PLP synthesis gene yaaDE into *E. coli* BL-BADE (pETDuet-*pelB-cadB-cadA*), which can produce 250 g L^{-1} cadaverine finally (productivity: 62.5 g L^{-1} h^{-1}). The addition of the inducer isopropyl β-D-1-thiogalactopyranoside (IPTG) and the enzyme co-factor PLP increases the cost for the whole cell bioconversion of L-lysine to cadaverine during the enzyme induction and catalytic process.[21,22] Currently, a new PLP- and IPTG-free whole cell bioconversion process of L-lysine to cadaverine has been developed by the engineered strain *E. coli* XL1-Blue (pKE112-HaLdcC) using lysine decarboxylase from *Hafnia alvei*. This recombinant XBHaLDC can produce 123.2 g L^{-1} cadaverine after 12 h of reaction with a productivity of 10.3 g L^{-1} h^{-1}.[21] These recombinant strains with CadA/mutant CadA/HaLdcC can improve either the stability or the activity of the enzymes; however, due to the low productivity of the enzyme, it is still difficult to meet the industrial requirement. Undoubtedly, we need to discover more efficient lysine decarboxylases for high-level cadaverine production.

In this study, we have first set up the databases with lysine decarboxylase protein sequences. For this, peptide pattern recognition (PPR) bioinformatic program[23,24] was used for discovering new lysine decarboxylases. Combined with the phylogenetic tree, sequence, and 3D structure analysis, nine lysine decarboxylases from different origins were further chosen for constructing the recombinant strains. After the characterization and optimization, we found an efficient lysine decarboxylase LdcEt from *Edwardsiella tarda*, which can completely convert 2 M L-lysine HCl to cadaverine with the productivity of up to 103.47 ± 4.37 g L^{-1} h^{-1}. This new lysine decarboxylase has great potential for large scale applications.

Results and discussion

Analysis of lysine decarboxylases by PPR

PPR is a non-alignment-based method for analyzing a large number of divergent protein sequences with a low degree of similarity.[23,24] In this study, 17 560 lysine decarboxylases (EC

4.1.1.18) protein sequences were downloaded from GenBank and then, 9901 curated protein sequences with less than 98% identity were used to create the peptide patterns with the PPR algorithm. The 9901 lysine decarboxylase protein sequences were divided into 57 groups based on the unique and conserved short peptides. The 57 short peptide groups can be combined with the homology to peptide pattern (Hotpep) to further identify the targeted lysine decarboxylase.[23] The muscle alignment of the highest scoring sequence in each PPR group and the percent identity matrix indicated that the 57 PPR groups were quite different (Fig. S1†). The phylogenetic tree of the sequences with the highest score in each PPR group showed that groups 1, 2, 4, 6, 26, 29, 45, 48, and 52 clustered closely together (Fig. S2†). Therefore, these 9 PPR groups provided more chances to find potential lysine decarboxylases. Further, the analysis of the 9 PPR groups indicated that constitutive lysine decarboxylases were mainly assigned to the PPR groups 2, 4, 6, 29, 48, and 52. PPR group 26 contained by far the most inducible lysine decarboxylases. Sequences that fell into groups 1 and 45 were not identified as constitutive or inducible lysine decarboxylases. It has been reported that inducible lysine decarboxylase has a much higher expression level, catalytic activity, and thermostability than the constitutive ones, which were progressively inactivated when the incubation temperature was above 37 °C.[25,26] Therefore, lysine decarboxylases from groups 1, 26, and 45 are the most interesting for further analysis according to the clustering analysis and the characterized sequences.

The 87 inducible lysine decarboxylases sequences in PPR group 26 were mainly originated from *E. coli*, *Klebstella* sp., *Serratia* sp., *Hafnia* sp., *Edwardsiella* sp., *Vibrio* sp., and *Aeromonas* sp. One genus clustered closely together except the sequences from *Edwardsiella* sp., which can be found in three clades (Fig. 1). The sequences from each genus with the highest score were isolated for further analysis (Table 1).

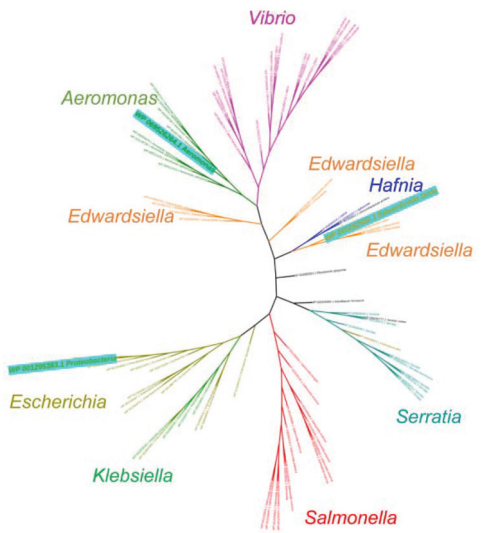

Fig. 1 Inducible lysine decarboxylases sequences in the PPR group 26.

Table 1 The predicted lysine decarboxylases based on the PPR and phylogenetic analysis

PPR group	Accession no.	Origin	Template	Seq. identity	Oligo-state	QSQE	Found by	Method	Resolution	Seq. Similarity	Range	Coverage
26	WP_001295383.1	*Proteobacteria*	3q16.1.A	100	Homo-10-mer	0.65	HHblits	X-ray	4.10 Å	0.61	1–711	1
	WP_095123982.1	*Klebsiella*	3q16.1.A	94.41	Homo-10-mer	0.65	HHblits	X-ray	4.10 Å	0.6	1–711	1
	WP_001100654.1	*Salmonella bongori*	3q16.1.A	92.44	Homo-10-mer	0.67	BLAST	X-ray	4.10 Å	0.59	1–711	1
	WP_020828344.1	*Serratia*	3q16.1.A	89.33	Homo-10-mer	0.69	BLAST	X-ray	4.10 Å	0.58	1–711	1
	WP_025800207.1	*Hafniaceae*	3q16.1.A	87.92	Homo-10-mer	0.67	BLAST	X-ray	4.10 Å	0.58	1–711	1
	WP_005282982.1	*Edwardsiella tarda*	3q16.1.A	86.83	Homo-10-mer	0.67	HHblits	X-ray	4.10 Å	0.57	1–711	1
	WP_069526264.1	*Aeromonas*	3q16.1.A	75.77	Homo-10-mer	0.59	HHblits	X-ray	4.10 Å	0.53	1–710	1
	WP_001229857.1	*Vibrio cholerae*	3q16.1.A	75.25	Homo-10-mer	0.6	HHblits	X-ray	4.10 Å	0.54	23–733	0.97
1	WP_086063064.1	*Bordetella*	2vyc.1.A	39.07	Homo-10-mer	0.49	HHblits	X-ray	2.40 Å	0.4	6–752	0.97
45	WP_062063161.1	*Cellvibrio*	1ord.1.A	29.84	homo-dimer	0.6	HHblits	X-ray	3.00 Å	0.36	26–750	0.93

Multisequence alignment showed that the catalytic active site, PLP-binding site, and the substrate combing site were highly conserved among these sequences (Fig. S3†). The sequence identity was in the range of 75.25–94.41% when compared with the well-studied CadA (WP 001295383.1) and the sequences were separated from each other based on the clustering analysis (Fig. 1).

Finally, the highest score sequence WP 086063064.1 from *Bordetella* sp. 8 (LdcBor) in group 1, WP 062063161.1 from *Cellvibrio* sp. OA-2007 (LdcCel) in group 45, and 7 sequences from *E. coli* (CadAEc), *Klebstella* sp. (LdcKle), *Salmonella bongori* (LdcSal), *Serratia* sp. (LdcSer), *Hafnia* sp. (LdcHaf), *Edwardsiella tarda* (LdcEt), *Vibrio* sp. (LdcVib), and *Aeromonas* sp. (LdcAer) in group 26 were chosen for further recombinant strain construction. Among them, the enzymes from *E. coli* (CadA),[18,25] *Klebstella* sp.,[27] *Hafnia* sp.,[21,28] and *Vibrio* sp.[29,30] were well-characterized. There will be significant space to explore the potential properties of the lysine decarboxylases from *Bordetella* sp., *Cellvibrio* sp., *Serratia* sp., *E. tarda*, *Salmonella* sp., and *Aeromonas* sp. according to the PPR prediction and the phylogenetic analysis.

Heterologous expression of the predicted lysine decarboxylases

The whole-cell bioconversion for cadaverine production is a promising process, which is suitable for large scale application. Ma *et al.*[13] found that fusing the signal peptide *pel*B to lysine/cadaverine antiporter (CadB) can overcome the permeability of the cell membrane and increase the cadaverine yield by 12%. Therefore, in this study, the codon optimized 9 genes and CadB fusing the signal sequence *pel*B was inserted to the pETDuet plasmid. The resulting pETDuet-ΔLDC-*pel*B-*cad*B was transferred to *E. coli* BL21 (DE3) for each lysine decarboxylase. The well-characterized CadA from *E. coli* was also included in this study. The recombinant strains were further cultured and induced for expressing the enzymes. All the genes (except LdcVib) were expressed according to the SDS-PAGE analysis (Fig. 2A). The molecular weight of these sequences (monomer) was close to 80 kDa for each enzyme.

The results of whole cell conversion of L-lysine HCl are available in Fig. 2B. LdcBor from *Bordetella* sp. 8 in PPR group 1 and LdcCel from *Cellvibrio* sp. in PPR group 45 did not show the decarboxylate activity when using L-lysine HCl as the substrate. It is interesting to find that lysine decarboxylase from *Edwardsiella tarda* (LdcEt) and *Aeromonas* sp. (LdcAer) in the PPR group 26 have much higher activity than the most studied CadAEc. These two enzymes have not been characterized yet. The cells with enzymes from *Salmonella bongori* (LdcSal) and *Hafnia* sp. (LdcHaf) have comparable catalytic component in the cells with CadAEc. Even though the lysine decarboxylase originating from *Hafnia* sp. has been investigated by protein engineering and heterologous expression to improve the cadaverine production,[21,28] its cadaverine productivity was not high enough for large scale application. In this study, the two enzymes LdcEt and LdcAer have been further analyzed for efficient cadaverine production.

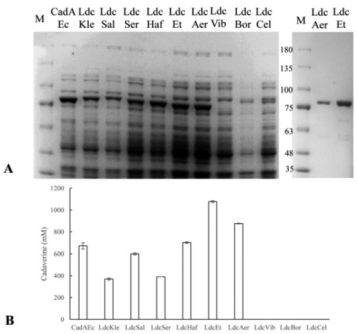

Fig. 2 (A) SDS-PAGE profile for the selected lysine decarboxylases. Lane 1 M (marker), lane 2 CadAEc from *E. coli*, lane 3 LdcKle from *Klebstella* sp., lane 4 LdcSal from *Salmonella bongori*, lane 5 LdcSer from *Serratia* sp., lane 6 LdcHaf from *Hafnia* sp., lane 7 LdcEt from *Edwardsiella tarda*, lane 8 LdcAer from *Aeromonas* sp., lane 9 LdcVib from *Vibrio* sp., lane 10 LdcBor from *Bordetella* sp., and lane 11 LdcCel from *Cellvibrio* sp. Purified LdcAer and LdcEt are shown in lane 12 and 13, respectively. (B) Whole cell conversion of 1.5 M L-lysine HCl to cadaverine by the recombinant host with the predicted lysine decarboxylases at pH 6, 45 °C, 500 rpm for 1 h.

Structural analysis of LdcEt and LdcAer

The 3D modeling homodecamer structures of LdcEt and LdcAer can be found in Fig. 3A and D. In the alignment for LdcEt, 710 of 714 target residues (99.4%) were aligned to template the residues (3N75, X-ray crystal structure of CadA). Among these aligned residues, the sequence identity and similarity were 86.8% and 93.8%, respectively. After the side-chains had been built, optimized, and fine-tuned, all newly modeled parts were subjected to a combined steepest descent and simulated annealing minimization. The overall quality *Z*-score (−0.388) of the resulting half-refined model indicated that the model quality was good. During the LdcAer homology modeling process, 709 of 710 target residues (99.9%) were aligned to the template residues (3N75). Among these aligned residues, the sequence identity is 75.6% and the sequence similarity is 86.2%. The full refined model with an overall quality *Z*-score of −0.403 was predicted as the final model. The unit of the LdcEt and LdcAer homodecamer was assembled by the two-fold symmetric dimer and the core domains including the linker region, PLP-binding domain, and subdomain 4 of each monomer were tightly associated, while the N-wing domains are separate from the body of the dimer as the described CadA structure (3N75).[15]

Lysine decarboxylases belong to the fold type I family of PLP-dependent enzymes, which need cofactor PLP to decarboxylate the α-carbonyl group of the substrate. It is important to identify the crucial contacts between the residues and PLP. In this study, 25 VINA docking runs of PLP to the receptor LdcEt and LdcAer were done at the optimal reaction pH 7 and 6, respectively. After clustering the 25 runs, 6 distinct complex conformations (differing by at least 5.0 A heavy atom RMSD after superposing on the receptor) were obtained for both the receptors. The first conformation with the highest binding energy (6.10 and 6.64 kcal mol^{-1} for LdcEt and LdcAer, respectively) and lowest dissociation constant (34007348 and

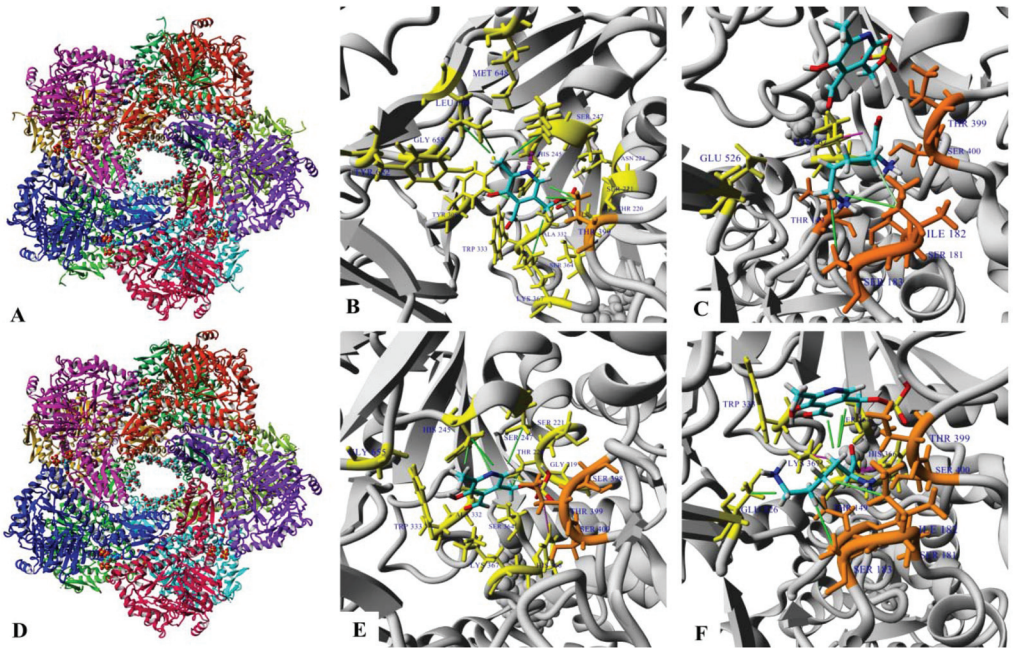

Fig. 3 3D model structure analyses of LdcEt and LdcAer. The 3D model homodecamer structure of LdcEt (A), PLP binding sites in LdcEt, PLP is shown as a stick with the color based on the element. Residues that directly interact with PLP are labeled and colored (B). The substrate coordinating sites in LdcEt. Both PLP and L-lysine are shown as sticks with the color based on the element. Residues that involve substrate binding are labeled and colored by yellow in one monomer and by orange in the second monomer. The hydrophobic interaction is shown in green line, the hydrogen bond is shown by the pink dotted line, and the ionic bond is shown by the pink line (C). The 3D model homodecamer structure of LdcAer (D), PLP binding sites in LdcAer (E), and the substrate coordinating sites in LdcAer (F).

13531609 pM for LdcEt and LdcAer, respectively) were shown in Fig. 3B and E. PLP contacted 16 LdcEt residues by hydrogen bonding with LYS246A and by hydrophobic interactions with HIS245, LYS246, TYR308A, LYS367, THR399 (residue from the second monomer), and LEU650. PLP participated in the interactions of 14 LdcAer residues (including the active site LYS367) by hydrogen bonding with GLY219, by hydrophobic interaction with THR220, HIS245, SER247, ALA332, THR399 (residue from the second monomer), and by ionic bonding with HIS366.

The residues involved in binding the substrate L-lysine during decarboxylation were further identified for both the enzymes (Fig. 3C and F). The binding active site LYS367 is in a cleft between the two monomers. The active site LYS367 contacted with L-lysine *via* ionic bonding. LYS367, GLU526 and THR149, SER181, ILE182, SER183, THR399, SER400 (from the second monomer) were also important for binding the substrate. It is interesting to find that LdcEt has a larger cleft for catalysis compared with that of LdcAer, which may result in higher catalytic activity for LdcEt (Fig. S4†). Kanjee *et al.*[15] have also proposed that LYS367 and GLU526 were important in coordinating the substrate binding. However, the residues involved in the decarboxylation process have still not been exactly clarified yet.

Characterization of the purified LdcEt and LdcAer

The enzymes with high thermostability, alkaline/acidic stability, and specific activity are highly desirable for industrial application. However, the most studied CadA from *E. coli* lose almost all the activity at pH 8.[25] In this study, the optimal pH for LdcEt and LdcAer was pH 7 and 6, respectively (Fig. 4A). LdcEt still has 40.88% and 18.66% activity when the reaction pH was 8 and 9, respectively. There was 23.46% activity for LdcAer at pH 8 (Fig. 4A). The pH profile for LdcEt was close to the alkaline lysine decarboxylase (AsLdc) from *Aliivibrio salmonicida* but the specific activity of LdcEt was 2.77 and 3.30 times higher when compared with AsLdc (optimal pH 7.5) and CadA (optimal pH 5.5), respectively.[26] The alkaline stability was further investigated for these two enzymes. The result showed that LdcEt was stable over the pH range of 5–7 after 24 h incubation. Also, it still has 28.44% residual activity after 24 h incubation at pH 8 (Fig. 4C). Surprisingly, LdcAer could retain 72.18% of its activity after 1 h incubation at pH 8 and still has 13.21% activity when it is incubated at pH 10 for 1 h (Fig. 4C). These two enzymes, which were active at elevated pH and relative alkaline stability, were highly desirable for industrial application as the product will increase the pH and less acid will be consumed in the reaction system.

Atomic force microscopy (AFM) was applied to track the morphological changes of the purified LdcEt when it was incubated at pH 5, 7, and 9 (Fig. 5). Fig. 5A showed that large aggregates have an assembled amount of LdcEt decamers present at pH 5.0 with the height of about 4.21 nm. The slight depolymerization of the large aggregates was observed at pH 7 and the height of the enzyme was similar to the large oligomers, indicating that the mixture of LdcEt decamers and oligo-

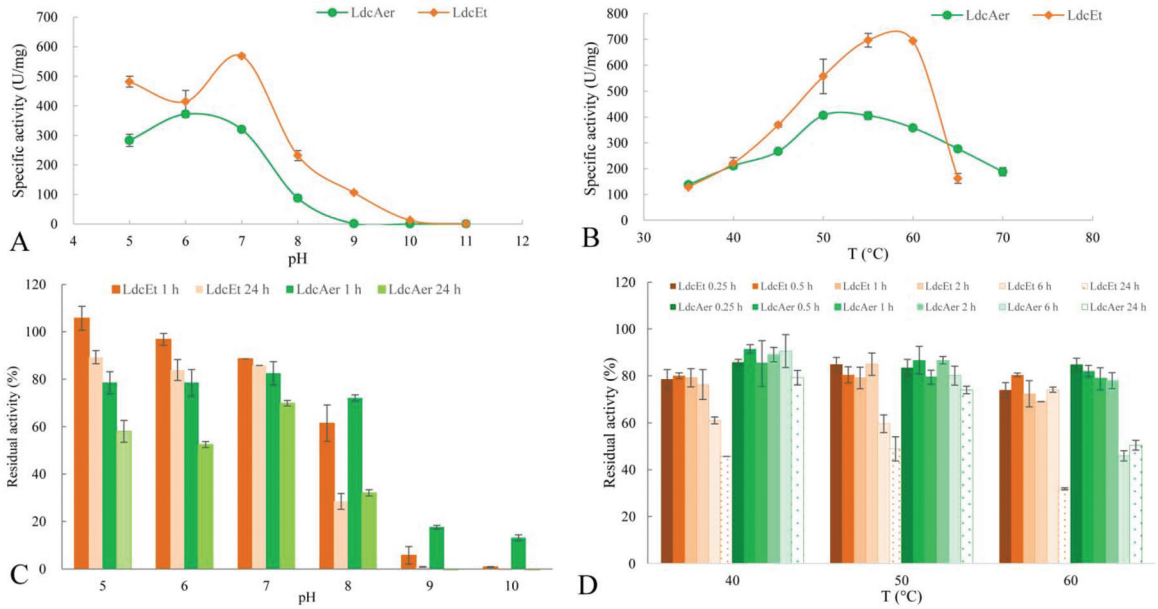

Fig. 4 Effects of temperature and pH on recombinant LdcEt and LdcAer activity and stability. (A) pH profile of LdcEt and LdcAer when using 10 mM L-lysine HCl as the substrate. (B) Temperature profile of LdcEt and LdcAer when using 10 mM L-lysine HCl as the substrate. (C) pH stability of LdcEt and LdcAer after incubating the enzyme under different pH for 1 h and 24 h, the residual activity was analyzed under the optimal condition using 10 mM L-lysine HCl as the substrate. (D) Thermostability of LdcEt and LdcAer, incubating the enzyme at 40, 50, and 60 °C for 15 min, 30 min, 1 h, 2 h, 6 h, and 24 h, the residual was is analyzed under the optimal condition using 10 mM L-lysine HCl as the substrate.

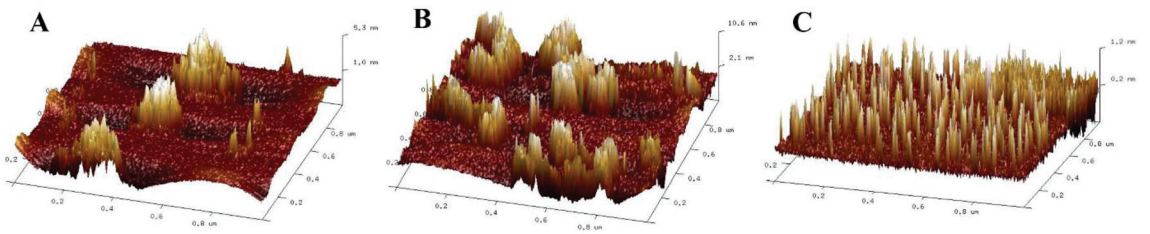

Fig. 5 The atomic force microscopy (AFM) images of LdcEt incubated at pH 5 (A), pH 7 (B), and pH 9 (C).

mers was still stable under this condition (Fig. 5B). However, the height of the enzyme decreased obviously when it was incubated under pH 9 (around 0.73 nm). Meanwhile, the size of the enzyme changed significantly when compared with the enzymes incubated at pH 5 and 7 (Fig. 5C). Therefore, the topological structure changes from pH 5 to 9, which demonstrated that LdcEt has a pH-dependent dissociation from large oligomers and decamers to dimers from pH 5 to 9 or even in an alkaline environment. The depolymerization of LdcEt will significantly affect the catalytic cleft between the two monomers, as described above. Hong *et al.*[18] designed the disulfide bond mutant together with the N-terminal region mutation of CadA; the resulting multimeric lysine decarboxylase (L7M/N8G/F14C/K44C) can improve the reaction pH from 4.9 to 8.3. The mutation (T88S) of CadA also exhibited higher reaction pH and alkaline stability when compared with the properties of wide-type CadA.[17] The half-rational/rational design of the interested enzymes has great potential for improving the enzymatic properties and for meeting the industrial requirement. In this study, LdcEt with high specific activity at elevated pH 7 and broad pH stability will have extremely high room to further improve its resistant properties so as to meet the industrial demand for the production of cadaverine.

Meanwhile, the advanced thermostability with the effective lifetime of the enzymes is also necessary for large scale application. The optimal reaction temperature for LdcEt and LdcAer was 55 and 50 °C, respectively (Fig. 4B). The specific activity of LdcEt and LdcAer was up to 696.39 U mg^{-1} and 406.29 U mg^{-1}, respectively, under the optimal pH and temperature. The thermostability results showed that both LdcEt and LdcAer were very stable when they were incubated at 40, 50, and 60 °C for 6 h. The residual activity of LdcEt and LdcAer, after incubation at 60 °C for 24 h, was 31.78% and 50.44%, respectively (Fig. 4D). LdcEt and LdcAer exhibited half-life of 14.5 h and 24.30 h at 60 °C, respectively. The half-life of the multimeric lysine decarboxylase (F14C/K44C) of CadA was 19 h

under 60 °C, increasing 216-folds when compared with the wide-type CadA.[18] The half-life of LdcEt and LdcAer was comparable with the mutation (F14C/K44C), indicating their high thermostability and effective lifetime, which most of the reported lysine decarboxylases cannot reach.[27,29,31]

We have also analyzed the purified enzymes and whole-cell bioconversion for catalyzing the high titer of the substrate (1.5 M L-lysine HCl) in the buffer with pH in the range of 5–11. However, the substrate has significant effects for the reaction pH and the initial pH was changed from 4.69 to 7.57 (Fig. S5A†). Though the cell will protect the enzymes and provide a better microenvironment for the reaction, the conversion by the cells and the purified enzyme have very similar pH and temperature profile for both LdcEt and LdcAer (Fig. S5A and S5B†). The main difference was that the activity decreased obviously at pH 11 for the cells as the cells were first suspended in the hash pH 11 condition, which damaged the function of the cells and affected the enzyme activity. Therefore, LdcEt and LdcAer can work efficiently in the high concentration of L-lysine HCl without adding the acid for controlling the pH, which will make the conversion process simple and economic.

The kinetic parameters of LdcEt and LdcAer can be found in Table 2. To our surprise, the maximal specific activity of LdcEt (1500 U mg^{-1}) and LdcAer (674.5 U mg^{-1}) was 10.3 and 4.6 times, respectively, which was higher than most studied CadA, which was 145.3 U mg^{-1}.[18] The k_{cat} of LdcEt and LdcAer was increased by 13.84 and 6.77 times, respectively (k_{cat} of CadA: 146.4 s^{-1}).[18] Though the K_m of LdcEt was higher than CadA and other lysine decarboxylases, the V_{max}, k_{cat}, and k_{cat}/K_m of this enzyme was far more than that of all the reported lysine decarboxylases, as shown in Table 2. The catalytic efficiency (k_{cat}/K_m) increased by 201% and 242% for LdcEt and LdcAer, respectively, when compared with CadA.[18] The specific activity of LdcEt (696.39 U mg^{-1}) was higher than that of LdcAer (406.29 U mg^{-1}) under the optimal conditions (Fig. 4B), showing the different result of catalytic efficiency (k_{cat}/K_m) for these two enzymes. The possible explanation was that the enzyme reaction rate was mainly controlled by k_{cat} but not K_m ($[S] \gg K_m$). The outstanding catalytic efficiency of LdcEt and LdcAer was highly important for efficient and economic cadaverine production.

Enhanced whole cell bioconversion of cadaverine

The whole cell bioconversion of L-lysine to cadaverine is a promising process for large scale application. However, the permeability of the cell wall and the cell membrane has great impact on the transfer rate of the substrate and the product.[32] The lysine/cadaverine antiporter CadB, which works based on the concentration gradients of L-lysine and cadaverine, was constructed and transformed to the host cell to improve the yield of cadaverine by 12%.[13] However, our study showed that the host cell co-expressing LdcEt and CadB (negative control in Fig. 6A) can still significantly improve the yield of cadaverine to 68.13% by cold pretreatment at −80 °C of the cells (positive control in Fig. 6A). The scanning electron microscopy (SEM) analysis also showed that the surface of the original cells (Fig. 7A) was obviously changed after cold pretreatment (Fig. 7C). However, −80 °C pretreatment of the cells makes the bioconversion process complex and uneconomical at the industrial scale for cadaverine production. Therefore, this study developed a new strategy for increasing the transfer rate of L-lysine and cadaverine. Different kinds of additives (solvents/detergents)[32] such as CTAB, SDBS, acetone, PEG600, Tween 80, anti-foamer, and Triton X-100 have been applied to the cadaverine whole cell bioconversion system. The results showed that the addition of 0.01% (v/v) of CTAB, SDBS, and Triton X-100 can increase the yield of cadaverine 1.14, 1.55, and 1.78 times, respectively (Fig. 6A), which were close to the positive control (−80 °C pretreatment of the cells). Kim *et al.*[33] have found that acetone can improve the whole cell conversion; however, acetone did not increase the yield of cadaverine, neither did PEG600 or the anti-foamer in this study. Different concentrations of CTAB, SDBS, and Triton X-100 were tested to further find the optimal additive and concentration. The results showed a the low concentration (0.005% (v/v)) of Triton X-100 was good enough to improve the transfer rate of L-lysine and cadaverine significantly (Fig. 6B).

SEM was employed to characterize the cell morphology. It was shown that the surface of the Triton X-100-treated cells

Table 2 Kinetic analysis of LdcEt, LdcAer, and other lysine decarboxylases based on the Michaelis–Menten equation

Enzyme	Origin	Reaction condition	K_m (mM)	k_{cat} (s^{-1})	k_{cat}/K_m (s^{-1} mM^{-1})	Ref.
CadA	*E. coli*	pH 6.5	0.42	30	71.43	15
CadA	*E. coli*	pH 5.6, 45 °C	1.22	146.4	120.1	18
CadA	*E. coli*	pH 5.5	0.78	—	—	26
CadA (L7M/N8G/F14C/K44C)	*E. coli*	pH 5.6, 45 °C	1.47	172.1	117.1	18
AsLdc	*Aliivibrio salmonicida*	pH 7.5	0.92	—	—	26
Ldc1E	Subtropical soil	pH 6.5, 40 °C	1.08	5.09	4.73	31
VvCadA	*Vibrio vulnificus*	pH 6, 37 °C	0.45	1.58	3.51	29
CadA	*Klebsiella pneumoniae*	pH 6, 37 °C	7.7	0.98	0.12	27
Ldc	*Selemonas ruminatium*	pH 6, 30 °C	1.5	16	10.66	34
Ldc	*Hafnia alvei*	pH 6.5, 37 °C	4.93	4.12	0.84	28
Ldc (E583G)	*Hafnia alvei*	pH 6.5, 37 °C	3.23	5.43	1.68	
L-Lys-DC	*Burkholderia* sp.	pH 6.0, 50 °C	0.84	—	—	35
LdcEt	*Edwardsiella tarda*	pH 7, 55 °C	8.41	2046	243.28	This study
LdcAer	*Aeromonas* sp.	pH 6, 50 °C	3.41	910	266.86	This study

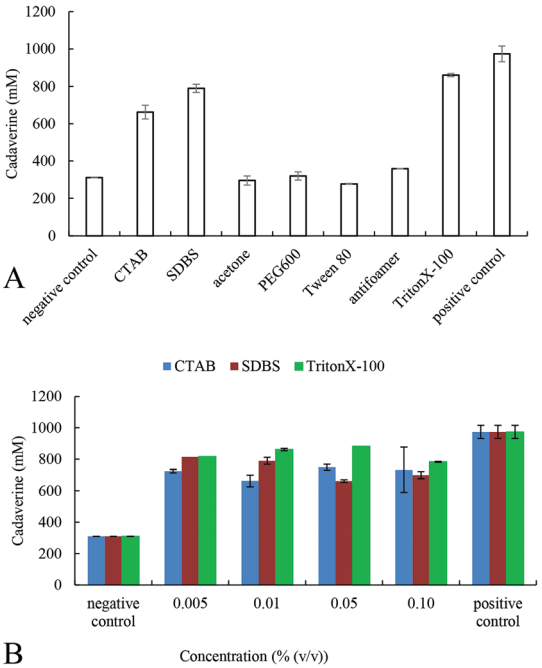

Fig. 6 Effect of additives on cadaverine production. Comparison of the final cadaverine yields after 1 h reaction in 1 M L-lysine HCl with 0.01% (v/v) 7 additives, the fresh cell without treatment were used as the negative control and the cells were kept at −80 °C for 2 h before the reaction, which was used as the positive control (A). Effects of different concentrations of CTAB, SDBS, and Triton X-100 on cadaverine production (B).

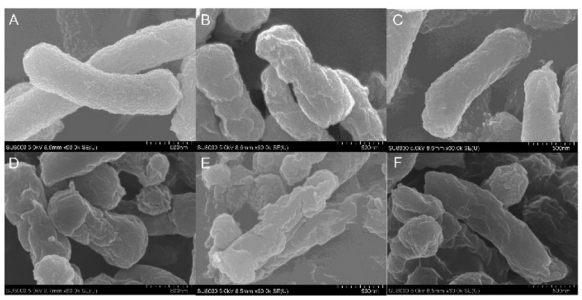

Fig. 7 Scanning electron microscopy (SEM) imaging of *E. coli* BL21 (DE3)/pETDuet-*ldc*Et-*pel*B-*cad*B. The fresh cells (A), cells after 1 h treatment by 0.01% (v/v) Triton X-100 (B), cells after being kept in −80 °C for at least 2 h (C), fresh cells after 1 h bioconversion of 1 M L-lysine HCl at pH 7, 55 °C (D), cells after the 1 h bioconversion of 1 M L-lysine HCl with the addition of 0.01% (v/v) Triton X-100 at pH 7, 55 °C (E), −80 °C frozen cells after the 1 h bioconversion of 1 M L-lysine HCl at pH 7, 55 °C (F).

(Fig. 7B) and cold-treated cells (Fig. 7C) were changed when comparing with the surface of the original cells (Fig. 7A), which can improve the transfer rate of the substrate and the product, resulting in the improvement of the catalytic efficiency. The membrane of the cells was almost excessively damaged by the product cadaverine, as shown in Fig. 7D, E, and F, which were the serious shortcomings for the reuse of the cells. The molecular modification of the membrane could be a strategy for designing the super host, which can resist the cadaverine effect and improve the membrane permeability limitation.

High level production of cadaverine by LdcEt and LdcAer

The high concentration of cadaverine will decrease the energy efficiency of the downstream separation and purification of the product. In this study, we used 2 M L-lysine HCl (365 g L^{-1}) (dissolved in 50 mM phosphate buffer, pH 8, the initial reaction pH was 6.45 as the pH was affected by the high concentration of L-lysine HCl) and the added cells (OD_{600} = 10, suspension in 50 mM phosphate buffer, pH 8) with −80 °C cold pretreatment (positive control), non-pretreatment (negative control), and the addition of 0.1% (v/v) Triton X-100 (cell treatment and bioconversion simultaneously). The reaction was performed at 50 °C without pH titration for the cells with LdcEt and LdcAer. It is interesting to find that the reactions containing the cells after cold pretreatment were severe and released large amount of bubbles in the first half hour. However, there were no bubbles in the reaction with the addition of Triton X-100. The addition of Triton X-100 to the reaction has outstanding function to improve the transfer rate of the cells with LdcEt, showing similar cadaverine productivity for the reaction with −80 °C cold pretreatment cells (Fig. 8A). The molar yield of cadaverine can reach 85% after 1 h conversion. Meanwhile, 2 M L-lysine HCl can be completely converted to cadaverine in 2 h. The cadaverine productivity was high up to 103.47 ± 4.37 g L^{-1} h^{-1}. Cells with LdcAer can completely convert 2 M L-lysine HCl in 4 h and its cadaverine productivity (50.06 ± 1.39 g L^{-1} h^{-1}) was lower than the cells with LdcEt (Fig. 8B). Whole cell conversion with LdcEt has the highest cadaverine productivity when compared with the most studied wild CadA and the mutations of all the published enzymes, as shown in Table 3. The high productivity of cadaverine and no pH control system can avoid using a large amount of acid for titrating the pH, which makes the *in vivo* bioconversion of the cadaverine process much easier to achieve and economical. Advanced expression systems without the necessity of IPTG induction and PLP addition can further improve the cost efficiency of the cadaverine production process.[21,22] The development of a new and economic system will be the part of ongoing research.

Then, half the amount of the cells (final OD_{600} = 5) were sonicated to obtain cell-lysates for high level L-lysine conversion. The resultant unpurified cell-lysates of LdcEt have almost the same capability to convert 2 M L-lysine HCl in 2 h as whole cell conversion even with for cell-lysates including the half amount of the cells (Fig. 8C). The unpurified cell-lysates of LdcAer can also produce 177.5 g L^{-1} cadaverine in 4 h (Fig. 8D). The results indicated that the cell-lysates of LdcEt have a relatively higher activity than whole cell conversion with LdcEt as the cell barrier has been completely avoided. The unpurified cell-lysates of LdcEt could be a promising and economic choice for the high level production of cadaverine at an industrial scale.

This study further applied purified LdcEt and LdcAer to convert the high concentration of L-lysine HCl (2 M) to cadaver-

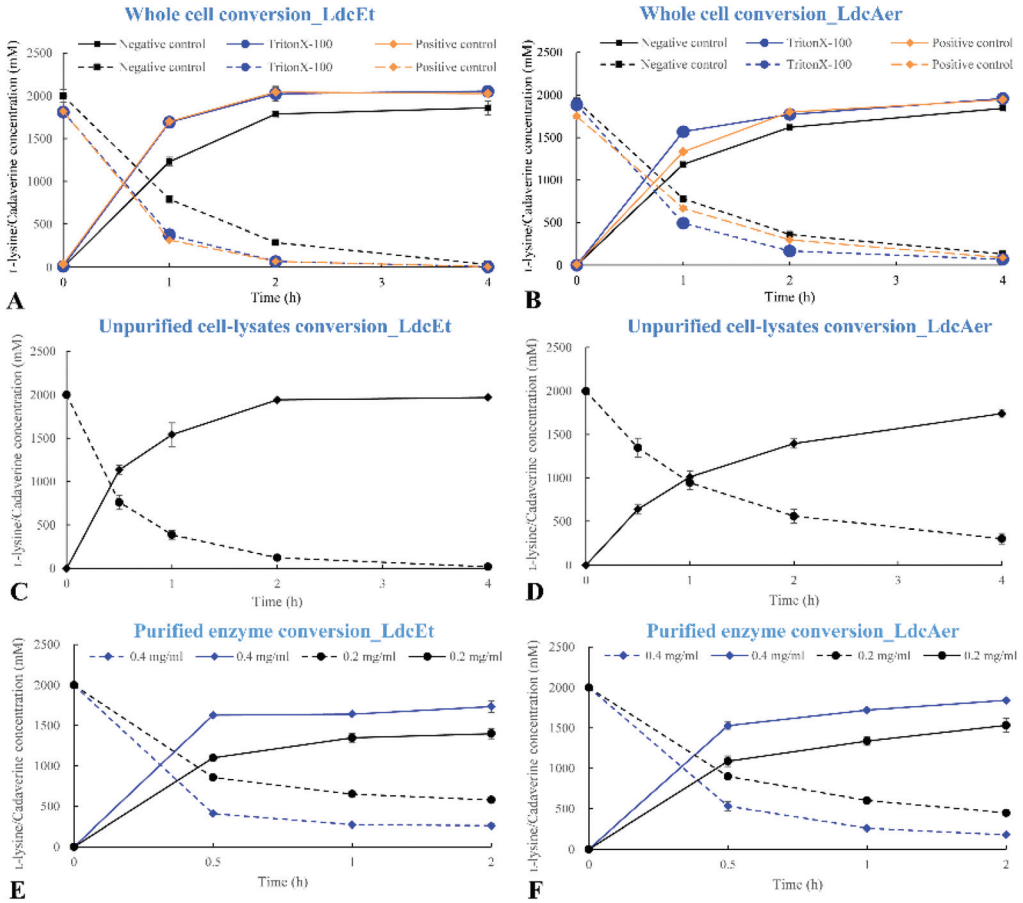

Fig. 8 High level production of cadaverine by LdcEt and LdcAer. Whole cell conversion of 2 M L-lysine HCl to cadaverine by the recombinant cells (OD_{600} = 10) with LdcEt (A) and LdcAer (B). Cells with −80 °C cold pretreatment (positive control), non-pretreatment (negative control), and the addition of 0.1% (v/v) Triton X-100 (cell treatment and conversion, simultaneously) were applied for whole cell conversion. Unpurified cell-lysate conversion of 2 M L-lysine HCl to cadaverine (the amount of cell-lysates is equal to the cells with the final OD_{600} as 5) by LdcEt (C) and LdcAer (D). Purified enzyme conversion of 2 M L-lysine HCl to cadaverine by 0.2 and 0.4 mg mL^{-1} purified LdcEt (E) and LdcAer (F). The full line shows the concentration of cadaverine and the dotted line shows the concentration of L-lysine.

Table 3 Production of cadaverine by the recombinant strains with lysine decarboxylases

Enzyme	Origin	Plasmid	Host	Cadaverine ($g\ L^{-1}$)	Productivity ($g\ L^{-1}\ h^{-1}$)	Ref.
CadA	*E. coli* BL21 (DE3)	pETDuet-*pelB*-*cadB*-*cadA*, pRSF-*yaaDE*	*E. coli* BL21(DE3)	250	62.5	36 and 37
CadA	*E. coli* K12 MG1655	pET23a-*cadA*	*E. coli* BL21(DE3)	Increased 80% of the yield	—	18
CadA	*E. coli* K12 W3110	pET28a-*cadA*	*E. coli* BL21(P_{T7}cadB)	200.2	66.7	38
HaLdcC	*Hafnia alvei*	pKE112-HaLdcC	*E. coli* XL1-Blue	136	1.13	19
LdcC	—	pT-cI^{ts}857-p_R-p_L-*pelBs-ldcC*	41#	116.8	29.2	39
CadA	*E. coli* BL21 (DE3)	pETDuet-*pelB*-*cadB*-*cadA*	*E. coli* BL21(DE3)	221	13.8	13
CadA(M176V/Y230H/K44R)	*E. coli* K12 MG1655	pET21-CadAM176 V/Y230H/K44R	*E. coli* BL21(DE3)	249	62.25	40
CadA(F14C/K44C/L7M/N8G)	*E. coli* B	pET24ma-CadAF14C/K44C/L7M/N8G	*E. coli* BL21(DE3)	157	16.53	18
CadA	*E. coli* K12 MG1655	pET21a-CadAM176V/Y230H/K44R	*E. coli* BL21(DE3)	198	39.6	17
Ldc(E583G)	*H. alvei* AS1.1009	pTrc99a-E583G	*E. coli* JM109	63.9	9.13	28
CadA(V3I/A590T)	*E. coli* K12 W3110	pUC19-CadAV3I/A590T	*E. coli* JM109	135	8.44	16
CadA	*E. coli* K12 MG1655	pSIT-Duet-*cadA*-*pelB*-*cadB*	*E. coli* BL21(DE3) ΔspeE, ΔspeG, ΔygjG&ΔpuuA	32.1	0.8	14
LdcEt	*Edwardsiella tarda*	pETDuet-*ldcEt*-*pelB*-*cadB*	*E.coli* BL21(DE3)	204	103.47 ± 4.37	This study
LdcAer	*Aeromonas* sp.	pETDuet-*ldcAer*-*pelB*-*cadB*	*E.coli* BL21(DE3)	204	50.06 ± 1.39	This study

ine. The results showed that both purified LdcEt and LdcAer can efficiently produce 165.96 ± 1.41 g L^{-1} and 155.84 ± 4.63 g L^{-1} at the initial pH of 7, 55 °C and initial pH of 6, 50 °C, respectively, by only 0.5 h and a very low dosage of enzyme (0.4 mg mL^{-1}) (Fig. 8E and F). We also found that 0.029 mg mL^{-1} LdcEt can completely convert 100% 1.5 M L-lysine HCl to cadaverine in 1 h. This was the first report of the significantly high catalytic efficiency of purified lysine decarboxylases LdcEt and LdcAer under such a high substrate concentration. Both the purified enzymes can tolerate more than 155 g L^{-1} cadaverine without pH control and work at higher than 50 °C, which can increase the solubility of the substrate. Kind *et al.*[41] reported that about 30 mM cadaverine (3.06 g L^{-1}) can reduce about 50% of the lysine decarboxylase activity. Therefore, the super properties for LdcEt and LdcAer were important for enhancing the yield of cadaverine by the *in vitro* reaction.[18,42]

Conclusions

In this study, we performed the comprehensive peptide-based bioinformatic analysis of the lysine decarboxylases by using PPR in combination with the phylogenetic relationship of the enzymes and the taxonomic position of the producing organism. Nine potent lysine decarboxylases were further investigated by heterologous expression and characterization. Two outstanding LdcEt and LdcAer from *Edwardsiella tarda* and *Aeromonas* sp., respectively, were stable over a broad range of pH (pH 5–7) and also have good thermostability with a half-life of 14.5 h and 20.3 h, respectively, at 60 °C. The kinetic analysis showed that they have the highest catalytic efficiency compared to that described earlier when compared with other studies. The recombinant cells and the cell-lysates also showed excellent capability for high-level production as it can completely convert 2 M L-lysine HCl to cadaverine in 2 h (productivity 103.47 ± 4.37 g L^{-1} h^{-1}). The low dosage of purified LdcEt and LdcAer (0.4 mg mL^{-1}) can also efficiently produce 165.96 ± 1.41 g L^{-1} and 155.84 ± 4.63 g L^{-1} in only 0.5 h. In conclusion, this study discovered new lysine decarboxylases with high specific activity, pH, thermostability, and catalytic efficiency *in vivo* and *in vitro*, and developed the process for simultaneous cell treatment *via* Triton X-100 and conversion, leading LdcEt to have a significant opportunity for the high-level production of cadaverine at an industrial scale.

Experimental section

Peptide pattern recognition analysis of the sequences of lysine decarboxylases

17 560 lysine decarboxylases (EC 4.1.1.18) protein sequences were downloaded from GenBank on 2019 July 11. Of these, 9901 not-identical sequences were identified (less than 98% identity between the sequences). These sequences were clustered in 57 unique PPR groups based on the unique and conserved short peptides using the same approach as that described for CAZymes.[23,24] The patterns can be used for finding additional lysine decarboxylases combined with the homology to peptide pattern (Hotpep) algorithm.[23]

Phylogenetic analysis

Phylogenetic analyses were performed for the top ranking lysine decarboxylase protein sequence in 57 unique PPR groups and 87 protein sequences of inducible lysine decarboxylases in PPR group 26. The WAG with Freqs. (+F) model and Jones-Taylor-Thornton (JTT) model was chosen, based on the best model prediction by MEGA-X. Nearest-Neighbor-Interchange (NNI) ML Heuristic Method was used for tree inference analysis. The Maximum Likelihood phylogenetic tree was finally constructed according to the manual of MEGA-X.[43] The trees were visualized in ITOL.[44]

Sequence and structure analysis

3D structures of LdcEt and LdcAer were predicted by YASARA's homology modeling experiment, Version 19.12.14.W.64[45] (YASARA Structure, YASARA Biosciences, Vienna, Austria), using the homology modelling function. The modeling speed was "Slow", and 10 and 15 possible templates were identified for LdcEt and LdcAer, respectively, by running 3 PSI-BLAST iterations to extract the position specific scoring matrix (PSSM) from UniRef90, then searching the PDB for a match (*i.e.*, hits with an E-value below the homology modeling cutoff 0.5). LdcEt and LdcAer shared the templates 3N75, 6Q7L, 5FKZ, and 2VYC, which were automatically identified as templates for the preparation of the homology models. LdcAer has one more template 5XX1. Finally, YASARA tried to combine the best parts of the predicted models to obtain a hybrid model, hoping to increase the accuracy beyond each of the contributors. However, the hybrid model could not be improved by copying parts from other models. The hybrid model was discarded, and edw_3n75-~01.yob and aer_3n75-~.yob were saved as the final model for LdcEt and LdcAer, respectively. After the side-chains had been built, optimized, and fine-tuned, all the newly modeled parts were subjected to a combined steepest descent and simulated annealing minimization. The *Z*-score was evaluated for the resulting half-refined and full unrestrained simulated annealing minimization. Finally, the half-refined model and fully refined model were accepted for LdcEt and LdcAer, respectively.

The final models of LdcEt and LdcAer were applied for ligand PLP docking around the active residue LYS367 under the optimal pH 7 and 6, respectively. PLP was cleaned and followed by an energy minimization step. 25 VINA docking runs of PLP to the receptor LdcEt/LdcAer yielded 6 clusters for both the enzymes. The binding energy (kcal mol^{-1}), dissociation constant (pM), and the contacting receptor residues were considered for choosing the clusters. Finally, the first cluster was applied for further research into LdcEt and LdcAer. Then, LdcEt_PLP and LdcAer_PLP were used for substrate L-lysine HCl superposition under optimal pH 7 and 6, respectively.

Heterologous expression of the predicted lysine decarboxylases

The genes of LdcEt (accession no. WP 005282982.1) and cadaverine/lysine antiporter (CadB, accession no. WP 000092909.1) were codon-optimized and synthesized by Shanghai Generay Biotechnology company. LdcEt and CadB genes were inserted into the NcoI/SacI and BglII/PacI restriction sites of the pETDuet plasmid, respectively, to construct the plasmid pETDuet-*ldc*Et-*cad*B. Then, the signal peptide pelB was introduced into the NdeI/BglII restriction site before CadB to construct the eventual expression vector pETDuet-*ldc*Et-*pel*B-*cad*B. Finally, the expression vector pETDuet-*ldc*Et-*pel*B-*cad*B was transferred into *E. coli* BL21 (DE3). The LdcEt gene was replaced by other codon-optimized lysine decarboxylase genes (LdcBor, LdcCel, CadAEc, LdcKle, LdcSal, LdcSer, LdcHaf, LdcVib, LdcAer) (Table 1) to construct different recombinant strains.

The recombinant strains were inoculated in 5 mL of LB medium containing 100 mg L^{-1} ampicillin, which were incubated at 37 °C for 12 h. Then, 1% of the culture was inoculated into 50 mL of LB medium containing 100 mg L^{-1} ampicillin at 37 °C, 200 rpm for 3 h. 0.1 mM IPTG was added for inducing the enzyme at 20 °C for 16–20 h. Finally, the cells were collected by centrifugation (6000 rpm, 5 min under 4 °C) and stored at −80 °C or used for whole-cell conversion directly.

Purification of lysine decarboxylase

The lysine decarboxylase was purified by fast protein liquid chromatography (FPLC) on an ÄKTA™ pure 25 with a 5 mL HisTrap HP crude affinity column (17524802, Cytiva) and 5 mL HiTrap desalting column (17140801, Cytiva), as described by Huang *et al.*,[46] with some modification. The frozen cells were suspended in the binding buffer (20 mM sodium phosphate, 0.1 mM PLP, 500 mM NaCl, 20 mM imidazole, pH 7.5) and the concentrated sample was obtained by cell sonication (power 60%, start 2 s, stop 3 s) for 30 min. 5 mL HisTrap HP crude affinity column was equilibrated with the binding buffer for 5 column volumes. Then, the concentrated sample was loaded into the column, followed by washing with the binding buffer for 5 column volumes. The column was gradient eluted with an elution buffer (20 mM sodium phosphate, 0.1 mM PLP, 500 mM NaCl, 500 mM imidazole, pH 7.5). The purified enzymes were collected and the elution buffer was replaced with the protein buffer (20 mM sodium phosphate, 0.1 mM PLP, 150 mM NaCl, 10% glycerol, pH 7.5) *via* the desalting column. The protein purity of lysine decarboxylase was determined by SDS-PAGE. The protein concentration of the purified lysine decarboxylase was analyzed according to the Pierce™ BCA Protein Assay Kit (23227, Thermo Scientific) and BSA used as the standards. Purified LdcEt and LdcAer were stored in protein buffer (20 mM sodium phosphate, 0.1 mM PLP, 150 mM NaCl, 10% glycerol, pH 7.5) with the concentration of 4–6 mg mL^{-1} in small aliquots at −80 °C.

Lysine decarboxylase activity analysis

Lysine decarboxylase activity was analyzed by using purified LdcEt and LdcAer: the reaction system was 500 μL in volume, including 10 mM L-lysine HCl, 0.1 mM pyridoxal phosphate (PLP), 0.12 μg purified enzyme, 50 mM phosphate buffer pH 7 or 50 mM sodium acetate buffer pH 6, which was incubated at 55 °C or 50 °C for 1 h for LdcEt and LdcAer, respectively. Then the reaction system was terminated at 70 °C for 5 min, and the sample was applied for L-lysine and cadaverine analysis.

The lysine decarboxylase activity was analyzed by using the recombinant cells with LdcEt and LdcAer: the frozen/fresh cells were suspended in 50 mM phosphate buffer pH 8. The suspended cells with the final OD_{600} 1.5 were added to the reaction system with the final 500 μL volume including 1 M L-lysine HCl, 0.1 mM pyridoxal phosphate (PLP), and 50 mM phosphate buffer pH 8, which was incubated at 55 °C or 50 °C for 1 h for the cells with LdcEt and LdcAer, respectively. Then the reaction system was terminated at 70 °C for 5 min and centrifuged at 12000 rpm for 2 min to obtain the supernatant for L-lysine and cadaverine analysis.

L-Lysine and cadaverine analysis by HPLC

L-Lysine and cadaverine were analysed by a high performance liquid chromatograph (HPLC, LC-ADXR, Japan), as described by Kim *et al.*,[47] with some modifications. The samples were firstly derivatized by diethylethoxymethylenemalonate (DEEMM) in the system including 600 μL 50 mM borate buffer (pH 9), 200 μL methanol, 130 μL distilled water, 60 μL diluted sample, and 10 μL of 1 M DEEMM. After incubation at room temperature for 10 min, the mixture was heated at 70 °C for 2 h to allow the complete degradation of excess DEEMM and the reagent by-products. Then, the sample was further analysed at 284 nm by reverse-phase chromatography on a C18 column (Shim-pack GIST-HP-C18 column, 2.1 × 100 mm, 3 μm particle size) at 35 °C. The eluent system comprised 100% acetonitrile (A) and 25 mM aqueous sodium acetate buffer (pH 4.8) (B), as well as a flow rate of 0.5 mL min^{-1} with the following gradient program: 0–2 min, 80–75% B; 2–27 min, 75–37.5% B; 27.01–37 min, 80% B. Quantification was performed using external standards of L-lysine and cadaverine.

Effects of temperature and pH on purified LdcEt and LdcAer

The optimal reaction pH of purified LdcEt and LdcAer was determined over a pH range of 5–11 (50 mM sodium acetate buffer pH 5, 6, 50 mM phosphate buffer pH 7, 8, 50 mM Tris hydrochloric acid buffer pH 9, and 50 mM sodium carbonate buffer pH 10, 11). The reaction system is the same as that for the session above (lysine decarboxylase activity analysis). The pH stability of the purified enzymes was analyzed by incubating the enzyme at different pH in the range of 5–11 at 4 °C for 24 h. The residual enzyme activity after 1 h and 24 h incubation was detected as described above.

The optimum reaction temperature of purified LdcEt and LdcAer was determined as described above except that the reactions were incubated at different temperatures (35–65 °C). The thermostability of the enzyme was also analyzed by incubating the purified enzymes for 24 h at 40, 50, and 60 °C in 50 mM sodium acetate buffer pH 5, and residual enzyme

activity after 1 h, 2 h, 6 h, and 24 h incubation was measured as described above.

Kinetic analysis

The Michaelis–Menten kinetics of purified LdcEt and LdcAer were determined using different concentrations of L-lysine HCl (0–25 mM) in 50 mM phosphate buffer pH 7 and in 50 mM sodium acetate buffer pH 6, respectively. 0.1 mM PLP and 0.468 μg purified LdcEt/LdcAer were added in the 500 μL reaction system. The enzyme reactions were carried out for 10 min under 55 and 50 °C for LdcEt and LdcAer, respectively. Then the reactions were terminated at 70 °C for 5 min. The k_{cat} and K_m were calculated by the enzyme kinetics-Michaelis–Menten method using the non-linear regression program GraphPad Prism 8 (https://www.graphpad.com/).

Effect of additives on cadaverine production

For the whole cell conversion system of LdcEt, 0.01% (v/v) hexadecyl trimethyl ammonium bromide (CTAB), sodium dodecyl benzene sulfonate (SDBS), acetone, PEG_{600}, Tween 80, antifoamer, and Triton X-100 were added. The reaction conditions were the same as in the above section "Lysine decarboxylase activity analysis". 0.005%, 0.01%, 0.05%, and 0.10% (v/v) of CTAB, SDBS, and Triton X-100 were further added to the whole cell conversion system. The frozen cells in the reaction system were applied as the positive control and the fresh cells in the reaction system without the additives were applied as the negative control.

Morphology analysis of the recombinant strain with LdcEt by scanning electron microscopy (SEM)

The surface morphology of the recombinant cells before and after whole cell conversion was investigated by SEM. The six samples included the cells before and after whole cell conversion: the fresh cells, cells after 1 h treatment with 0.01% (v/v) Triton X-100, cells kept at −80 °C for at least 2 h, fresh cells after bioconversion, fresh cells after bioconversion with the addition of 0.01% (v/v) Triton X-100, and −80 °C frozen cells after the 1 h bioconversion. The cells were washed three times with 50 mM phosphate buffered saline (pH 7.2). Subsequently, they were fixed for 8 h at 4 °C with 2.5% glutaraldehyde and then dehydrated by graded ethanol series (50%, 60%, 70%, 80%, 90%, and 100%, 10 min for each titer) and finally by pure *tert*-butanol (twice, 10 min for each time). Then, the samples were lyophilized, coated with gold, and visualized using a SEM-EDX SU8020 microscope.

Morphology analysis of LdcEt by atomic force microscopy (AFM)

LdcEt was incubated in pH 5, 7, and 9 for 1 h; the enzyme solution was then dropped on the fresh mica surface and dried using nitrogen at first. Then, the surface 2D and 3D topography of the protein was measured using AFM (Multimode, Bruker, USA) under the tapping mode. AFM tips (SNL-10) with nominal spring constants between 0.05 and 0.5 N m^{-1} were used throughout the experiments, and the scan rate was 1.00 Hz. The images underwent second-order flattening using Nanoscope Analysis.

High-level production of cadaverine

High-level production of cadaverine by whole cell conversion: the frozen/fresh cells were resuspended in 50 mM phosphate buffer pH 8. The 20 mL high-level production of cadaverine system included 2 M L-lysine HCl (364 g L^{-1}) and 0.1 mM PLP, which was resuspended with final OD_{600} as 10 and 50 mM phosphate buffer pH 8. The reaction system with the frozen cells was the positive control. The reaction system with 0.1%/0.5% (v/v) Triton X-100 and fresh cells was compared with the positive and negative control, with the reaction system containing the fresh cells but without 0.1%/0.5% (v/v) Triton X-100. After incubating at 50 °C for 1–4 h for cells with LdcEt and LdcAer, respectively, the whole-cell conversion system was terminated at 70 °C for 5 min and centrifuged to obtain the supernatant for cadaverine determination.

High-level production of cadaverine by unpurified cell-lysates conversion: the fresh cells were resuspended in 50 mM phosphate buffer pH 8 and the cell-lysates were obtained by cell sonication as described in the section "Purification of lysine decarboxylase". The 20 mL high-level production of cadaverine system included 2 M L-lysine HCl (364 g L^{-1}), 0.1 mM PLP, unpurified cell-lysates (the addition was equal to the cells with final OD_{600} as 5) and 50 mM phosphate buffer pH 8. After incubating at 50 °C for 0.5–4 h for the unpurified cell-lysates with LdcEt and LdcAer, respectively, the reaction was terminated at 70 °C for 5 min. The following experimental steps were the same as those above.

High-level production of cadaverine by purified enzyme conversion: The purified LdcEt and LdcAer were further applied for the high-level production of cadaverine. 0.2 mg per 0.4 mg LdcEt and LdcAer were added into the 1 mL reaction system including 2 M L-lysine HCl (364 g L^{-1}), 0.1 mM PLP, and 50 mM phosphate buffer pH 8 and pH 7, under 55 °C and 50 °C, respectively. The reactions were terminated at 70 °C for 5 min and diluted for cadaverine determination.

Conflicts of interest

There are no conflicts to declare.

Acknowledgements

This work was supported by the Innovation Academy for Green Manufacture, CAS (IAGM2020C19), Henan Key Research and Development Project (202102210046), Hebei Natural Science Foundation (B2020103010), Beijing Nova Program of Science and Technology (Z201100006820141), and the CAS Pioneer Hundred Program.

References

1 T. M. Carole, J. Pellegrino and M. D. Paster, *Twenty-Fifth Symposium on Biotechnology for Fuels and Chemicals*, Totowa, NJ, 2003.
2 S. Kind, S. Neubauer, J. Becker, M. Yamamoto, M. Volkert, G. Abendroth, O. Zelder and C. Wittmann, *Metab. Eng.*, 2014, **25**, 113–123.
3 D. Platt, *Eur. Plast. News*, 2004, **31**, 15.
4 K. Jo, H. J. Kim and H. H. Lee, *Fibers Polym.*, 2019, **20**, 63–68.
5 E. F. Gale and H. M. R. Epps, *Biochem. J.*, 1942, **36**, 600–618.
6 Z. G. Qian, X. X. Xia and S. Y. Lee, *Biotechnol. Bioeng.*, 2011, **108**, 93–103.
7 R. Matsuura, T. Tanaka and A. Kondo, *Basic Clin. Pharmacol.*, 2019, **124**, 17.
8 E. Sgobba, A. K. Stumpf, M. Vortmann, N. Jagmann, M. Krehenbrink, M. E. Dirks-Hofmeister, B. Moerschbacher, B. Philipp and V. F. Wendisch, *Bioresour. Technol.*, 2018, **260**, 302–310.
9 T. U. Chae, J. H. Ahn, Y. S. Ko, J. W. Kim, J. A. Lee, E. H. Lee and S. Y. Lee, *Metab. Eng.*, 2019, **58**, 2–16.
10 J. Cheng, P. Chen, A. Song, D. Wang and Q. Wang, *J. Ind. Microbiol. Biotechnol.*, 2018, **45**, 719–734.
11 S. Kind and C. Wittmann, *Appl. Microbiol. Biotechnol.*, 2011, **91**, 1287–1296.
12 N. Kiyohiko, E. Shuichi, M. Yukiko, T. Kazuhiko and H. Yoshinori, *US Pat.*, 2005003497, 2004.
13 W. Ma, W. Cao, H. Zhang, K. Chen, Y. Li and P. Ouyang, *Biotechnol. Lett.*, 2015, **37**, 799–806.
14 C. Y. Huang, W. W. Ting, Y. C. Chen, P. Y. Wu, C. D. Dong, S. F. Huang, H. Y. Lin, S. F. Li, I. S. Ng and J. S. Chang, *Biochem. Eng. J.*, 2020, **156**, 107514.
15 U. Kanjee, I. Gutsche, E. Alexopoulos, B. Zhao, M. El Bakkouri, G. Thibault, K. Liu, S. Ramachandran, J. Snider, E. F. Pai and W. A. Houry, *EMBO J.*, 2011, **30**, 931–944.
16 O. Fumito and M. Yasuhiro, *European Pat.*, 3118312B1, 2015.
17 F. Kou, J. Zhao, J. Liu, C. Sun, Y. Guo, Z. Tan, F. Cheng, Z. Li, P. Zheng and J. Sun, *Biotechnol. Lett.*, 2018, **40**, 719–727.
18 E. Y. Hong, S. G. Lee, B. J. Park, J. M. Lee, H. Yun and B. G. Kim, *Biotechnol. J.*, 2017, **12**, 1700278.
19 Y. M. Moon, S. Y. Yang, T. R. Choi, H. R. Jung, H.-S. Song, Y. H. Han, H. Y. Park, S. K. Bhatia, R. Gurav, K. Park, J. S. Kim and Y. H. Yang, *Enzyme Microb. Technol.*, 2019, **127**, 58–64.
20 W. Ma, W. Cao, B. Zhang, K. Chen, Q. Liu, Y. Li and P. Ouyang, *Sci. Rep.*, 2015, **5**, 10.
21 H. T. Kim, K. A. Baritugo, Y. H. Oh, K. H. Kang, Y. J. Jung, S. Jang, B. K. Song, I. K. Kim, M. O. Lee, Y. T. Hwang, K. Park, S. J. Park and J. C. Joo, *Polymers*, 2019, **11**, 1184.
22 J. Rui, S. You, Y. Zheng, C. Wang, Y. Gao, W. Zhang, W. Qi, R. Su and Z. He, *Bioresour. Technol.*, 2020, **302**, 122844.
23 P. K. Busk, B. Pilgaard, M. J. Lezyk, A. S. Meyer and L. Lange, *BMC Bioinf.*, 2017, **18**, 214.
24 P. K. Busk and L. Lange, *Appl. Environ. Microbiol.*, 2013, **79**, 3380–3391.
25 M. Lemonnier and D. Lane, *Microbiology*, 1998, **144**, 751–760.
26 F. Kou, J. Zhao, J. Liu, J. Shen, Q. Ye, P. Zheng, Z. Li, J. Sun and Y. Ma, *J. Mol. Catal. B: Enzym.*, 2016, **133**, S88–S94.
27 J. H. Kim, H. J. Kim, Y. H. Kim, J. M. Jeon, H. S. Song, J. Kim, S. Y. No, J. H. Shin, K. Y. Choi, K. M. Park and Y. H. Yang, *J. Microbiol. Biotechnol.*, 2016, **26**, 1586–1592.
28 C. Wang, K. Zhang, C. Zhongjun, H. Cai, W. Honggui and P. Ouyang, *Biotechnol. Bioprocess Eng.*, 2015, **20**, 439–446.
29 L. Han, J. Yuan, X. Ao, S. Lin, X. Han and H. Ye, *Front. Microbiol.*, 2018, **9**, 3082.
30 S. Jeong, Y. J. Yeon, E.-G. Choi, S. Byun, D. Cho, I. K. Kim and Y. H. Kim, *Korean J. Chem. Eng.*, 2016, **33**, 1530–1533.
31 J. Deng, H. Gao, Z. Gao, H. Zhao, Y. Yang, Q. Wu, B. Wu and C. Jiang, *PLoS One*, 2017, **12**, e0185060.
32 R. R. Chen, *Appl. Microbiol. Biotechnol.*, 2007, **74**, 730–738.
33 H. Kim, H. Y. Yoo, N. Park, H. Kim, J. Lee, Y. Baek, T. Lee, J. M. Oh, J. Cho and C. Park, *Polymers*, 2019, **11**, 1372.
34 Y. Takatsuka, Y. Yamaguchi, M. Ono and Y. Kamio, *J. Bacteriol.*, 2000, **182**, 6732–6741.
35 A. Sugawara, D. Matsui, N. Takahashi, M. Yamada, Y. Asano and K. Isobe, *J. Biosci. Bioeng.*, 2014, **118**, 496–501.
36 W. Ma, W. Cao, B. Zhang, K. Chen, Q. Liu, Y. Li and P. Ouyang, *Sci. Rep.*, 2015, **5**, 10.
37 K. Chen, W. Ma, Y. Qi, Y. He, J. Shen and P. Ouyang, *China Pat.*, 106148373A, 2016.
38 T. Wen, S. Liu, Y. Liang, Y. Zhang and X. Shang, *China Pat.*, 105316270B, 2014.
39 K. Tian, F. Lu and Z. Wang, *China Pat.*, 105368766A, 2015.
40 J. Sun, J. Zhao, J. Liu, C. Sun, P. Zhen and Y. Ma, *China Pat.*, 107164352A, 2017.
41 S. Kind, S. Kreye and C. Wittmann, *Metab. Eng.*, 2011, **13**, 617–627.
42 J. F. Rocha, A. F. Pina, S. F. Sousa and N. M. F. S. A. Cerqueira, *Catal. Sci. Technol.*, 2019, **9**, 4864–4876.
43 S. Kumar, G. Stecher, M. Li, C. Knyaz and K. Tamura, *Mol. Biol. Evol.*, 2018, **35**, 1547–1549.
44 I. Letunic and P. Bork, *Nucleic Acids Res.*, 2019, **47**, W256–W259.
45 E. Krieger and G. Vriend, *J. Comput. Chem.*, 2015, **36**, 996–1007.
46 Y. Huang, X. Zheng, B. Pilgaard, J. Holck, J. Muschiol, S. Li and L. Lange, *Appl. Microbiol. Biotechnol.*, 2019, **103**, 777–791.
47 Y. H. Kim, H. J. Kim, J. H. Shin, S. K. Bhatia, H. M. Seo, Y. G. Kim, Y. K. Lee, Y. H. Yang and K. Park, *J. Mol. Catal. B: Enzym.*, 2015, **115**, 151–154.